Influence of Protein Surface Charge on the Bimolecular Kinetics of a Potassium Channel Peptide Inhibitor†

Laura Escobar,‡ Michael J. Root, and Roderick MacKinnon*

Department of Neurobiology, Harvard Medical School, 220 Longwood Avenue, Boston, Massachusetts 02115

Received January 29, 1993; Revised Manuscript Received April 2, 1993

ABSTRACT: This study investigates the influence of a through-solution electrostatic interaction on the kinetics of ion channel blockade by the high-affinity peptide inhibitor Lq2. Membrane patches containing many Shaker K^+ channels were removed from *Xenopus* oocytes and placed in a rapid perfusion chamber. Lq2 association and dissociation rate constants were determined from the relaxations to equilibrium blockade following rapid changes in toxin concentration. The association and dissociation rate constants were 8.5 $\times 10^7$ M^{-1} s^{-1} and 0.71 M^{-1} s^{-1}, respectively, in 100 mM NaCl solution, pH 7.1, at room temperature (21–23 °C). Charge-altering mutations introduced at position 422 on the ion channel affect toxin affinity in a manner consistent with a through-solution electrostatic interaction. The full effect of the charge mutations is expressed kinetically on the association rate; toxin dissociation remains unaltered. An electrostatic influence on the association rate alone is expected if diffusion of toxin up to (and away from) its receptor on the channel is fast compared to the rate of formation of short-range contacts that are necessary to produce the bound state.

Many ion channels are inhibited by naturally occurring peptide toxins. Over the past decade, numerous peptide inhibitors of Ca^{2+}, Na^+, and K^+ channels have been discovered. These toxins are highly specific for their target ion channels, and they are effective at nanomolar concentrations. Because of their high specificity and high affinity, they have been very useful for pharmacologically distinguishing the different channels in a cell's membrane (Mintz et al., 1992), as well as for mapping the membrane folding topology using ion channel mutagenesis (Catterall, 1988; MacKinnon & Miller, 1989a; MacKinnon et al., 1990).

Peptide channel toxins are proving to be useful for another purpose: for studying the interaction between two proteins using high-resolution functional measurements (Moczydlowski et al., 1988; MacKinnon & Miller, 1989a; Park & Miller, 1992a,b; Giangiacomo et al., 1992, 1993). The aim of such studies is to understand how the toxin and channel make a high-affinity contact. What are the relevant forces that govern molecular recognition? The channel–toxin system is unique because one of the proteins, the ion channel, is fixed in a patch of membrane at the tip of a glass pipette. The channel's activity can therefore be monitored continuously since the channel mediates a measurable ionic current through the membrane patch. When a toxin molecule combines with the ion channel, the current is blocked. Thus, the current record provides a real-time measure of the ion channel–toxin interaction.

One class of peptide inhibitors of K^+ channels has been studied extensively over the past few years. Charybdotoxin (ChTX) is the best characterized member, but many isoforms have been described (Miller et al., 1985; Anderson et al., 1988; MacKinnon & Miller, 1988; Lucchesi et al., 1989; Gimenez-Gallego et al., 1988; Galvez et al., 1990; Smith et al., 1986; Garcia et al., 1991). The scorpion toxin inhibitors of K^+ channels are 37–39 amino acids in length, and they share 6 fully conserved cystine residues. The NMR structures of two of these toxins, ChTX (Botems et al., 1991) and iberiotoxin (IbTX) (Johnson & Snugg, 1992), have been determined. ChTX and IbTX have very similar structures as would be expected on the basis of their similar mechanism of action on K^+ channels. Studies on the mechanism of how these toxins inhibit a K^+ channel have revealed two prominent features of the blocking reaction. First, a toxin molecule binds with a 1:1 stoichiometry to a channel's outer mouth where it obstructs K^+ ion conduction (MacKinnon & Miller, 1988, 1989b; Miller, 1988; Giangiacomo et al., 1992). Second, there is a strong electrostatic attraction between the cationic toxin and the anionic mouth of the K^+ channel (Anderson et al., 1988; MacKinnon & Miller, 1989a).

This study focuses on the electrostatic interaction between one member of the ChTX family of scorpion toxins, Lq2, and a Shaker K^+ channel. Specifically, we ask how do mutations at one particular position on the ion channel influence the toxin association and dissociation rate constants. Previous work using a related toxin showed that altering a charge at a residue near the toxin binding site affected the *equilibrium* for inhibition in a manner consistent with a through-solution electrostatic interaction (MacKinnon & Miller, 1989a). How is through-solution electrostatic stabilization displayed in terms of the reaction *kinetics*? Is the association rate or the dissociation rate affected? To answer these questions, a rapid perfusion system has been developed in order to measure the kinetics of Lq2 inhibition of Shaker K^+ channels expressed in *Xenopus* oocytes. We find that mutations which alter the charge on the channel near the toxin binding site (at position 422) affect only the association rate and not dissociation. A through-solution electrostatic interaction that influences only the association rate can be most easily understood in terms of a bimolecular reaction that operates far from the diffusion-controlled limit.

MATERIALS AND METHODS

Materials. T4 DNA polymerase and DNA ligase were obtained from Bio-Rad (Richmond, CA), T7 RNA polymerase was from Promega (Madison, WI), nucleotide triphosphates

† This research was supported by NIH Grant GM43949. M.J.R. was supported by NRSA Grant T32 GM07753-14. L.E. received support from DGAPA and CONACYT.

‡ Present address: Unidad de Investigacion Biomedica, Centro Medico Nacional, IMMS, Mexico.

0006-2960/93/0432-6982$04.00/0 © 1993 American Chemical Society

were from Pharmacia (Piscataway, NJ), and restriction enzymes were from New England Biolabs (Beverly, MA). Enteropeptidase (EK2) was from Biozyme (San Diego, CA) and *Xenopus laevis* from Xenopus One (Ann Arbor, MI).

Preparation of Recombinant Lq2. Native Lq2 was purified from the venom of the scorpion *Leiurus quinquestriatus Hebraeus* (Latoxan; Rosans, France) according to a method described by Moczydlowski (Lucchesi et al., 1989). After it was established that Shaker K^+ channels were sensitive to Lq2, recombinant toxin was produced in bacteria using a procedure developed by Park et al. for the synthesis of ChTX (Park et al., 1990). All results presented here were carried out using the recombinant Lq2. An Lq2 gene was made from two synthetic oligonucleotide duplexes and inserted into the pCSP105 vector (Park et al., 1990). The vector was modified so that Lq2 could be cleaved from the fusion protein using enteropeptidase (Biozyme). The toxin was produced as a fusion protein in *Escherichia coli* strain BL21. Partial purification of the fusion protein involved ammonium sulfate precipitation and DEAE-cellulose column chromatography. After dialysis against 10 mM Tris-HCl, pH 7.0, 5 mM $CaCl_2$ and 200 units/mg of enteropeptidase were added, and the sample was incubated at 37 °C for 30 h. Rapid cyclization of the amino-terminal glutamine was favored by adding acetic acid (5%) and incubating at 65 °C for 4 h. The cleaved toxin was separated from the fusion protein on an SP-Sephadex C25 column. A final HPLC reverse-phase (C8) column was used to concentrate and collect a single Lq2 peak. The extinction coefficient for ChTX, 17 500 M^{-1} cm^{-1}, was used to calculate the final concentration of Lq2 (Smith et al., 1986). (ChTX and Lq2 are identical at 29 out of 37 amino acids. Aromatic residues Trp, Tyr, and Phe are fully conserved.)

Potassium Channel Mutagenesis and Expression. The Shaker H4 K^+ channel (Kamb et al., 1987), present in a Bluescript vector (Stratagene; LaJolla, CA), was modified by deleting amino acids 6–46 to remove fast inactivation (Hoshi et al., 1990) as we have described previously (Heginbotham & MacKinnon, 1992). (The amino acid numbering used here corresponds to the unmodified Shaker K^+ channel.) A mismatch oligonucleotide was used to introduce point mutations using a *dut⁻ ung⁻ selection method* (Kunkel, 1985), and the mutation was confirmed by sequencing the mutated region (Sanger et al., 1977). RNA transcription and *Xenopus* oocyte injections were carried out using previously described protocols (MacKinnon et al., 1988).

Electrophysiological Recording. Channels were expressed in *Xenopus* oocytes to a density such that a membrane patch usually contained between 100 and 1000 channels (0.1–1.0-nA K^+ current). The membrane potential was controlled and the current recorded using a commercial patch clamp amplifier (Axon Instruments). Patches were excised from the oocyte in an outside-out configuration, and the pipet tip was immediately moved into the stream of a flow chamber (Figure 1). By switching rapidly between separate solution inputs using solenoids under computer control, the toxin concentration at the pipet tip could be changed within 100 ms. The current trace in Figure 1 shows the dead time of the system when the input solution is switched to one containing the channel blocker TEA synchronously with the onset of membrane depolarization. TEA reaches the patch in about 50 ms. This delay was sufficiently short compared to the slow rate of equilibration of Lq2 with the channel so that no correction was necessary. Membrane patches were held at −100 mV where the channels are shut. Channels were opened by stepping to 0 mV for 20–50 ms repeatedly with a duty cycle of 1–4 Hz. A change in the fraction of channels activated during depolarization following the addition of toxin provides a direct measure of channel blockade which occurred prior to membrane depolarization. (The toxin binds to and inhibits even the shut channel.) In all experiments, the internal (pipet) solution (in millimolar) was 100 KCl, 5 $MgCl_2$, 5 EGTA, and 10 HEPES, pH 7.1 (KOH). The standard external (bath) solution (in millimolar) was 100 NaCl, 2 KCl, 5 $MgCl_2$, 1.8 $CaCl_2$, and 10 HEPES, pH 7.1 (NaOH). Where specifically indicated, ionic strength was changed by varying the bath NaCl concentration between 25 and 200 mM. To control osmolarity, 150 or 100 mM sucrose was added to all solutions containing 25 or 50 mM NaCl, respectively. All experiments were carried out at room temperature (21–23 °C).

One set of experiments (Figure 2) was carried out using a two-electrode voltage clamp amplifier to record from whole oocytes as previously described (MacKinnon et al., 1988). The bath solution was identical to that used in the patch recording experiments.

Data Collection and Analysis. Repeated current traces were recorded following the addition and removal of toxin. Data were filtered at 1 kHz, sampled at 5 kHz, and stored on a computer disk for subsequent analysis. Analysis showed monoexponential current relaxations to and from an equilibrium-blocked state following the addition or removal of toxin. The relaxations were fit (least-squared) to equations corresponding to the bimolecular reaction scheme

$$\text{unblocked channel} \underset{\beta}{\overset{\alpha[T]}{\rightleftharpoons}} \text{blocked channel}$$

where α is the second-order association rate constant, [T] the toxin concentration, and β the first-order dissociation rate constant. During the onset of blockade, the time constant for relaxation to equilibrium is

$$\tau_{\text{wash in}} = (\alpha[T] + \beta)^{-1} \quad (1)$$

and for recovery following removal of toxin, it is

$$\tau_{\text{wash out}} = \beta^{-1} \quad (2)$$

The equilibrium unblocked fraction of channels, I/I_0, is related to the rate constants and toxin concentration according to

$$I/I_0 = \beta/(\alpha[T] + \beta) \quad (3)$$

and so the desired quantities α and β are overdetermined.

RESULTS

The aim of this study is to understand how electrostatic forces can influence the kinetics of a bimolecular protein–protein interaction. Before addressing this central question, we first investigate the basic features of Lq2 blockade of Shaker K^+ channels since previous work has been carried out using a toxin isoform and not Lq2 itself. Figure 2 shows the unblocked fraction of channels (measured at equilibrium), I/I_0, as a function of the Lq2 concentration on the outside of an oocyte. The data points follow a single site binding function with an inhibition constant (K_i) of 7 nM (eq 3 with $\beta/\alpha = K_i$). The inhibition is fully reversed upon removal of toxin from solution.

We next ask if we can resolve the rates of Lq2 association and dissociation with its binding site on the channel. Figure 3 shows the results of an experiment in which a membrane patch was exposed to rapid changes in toxin concentration (see Materials and Methods). The patch contained many Shaker K^+ channels which opened with a characteristic time course during membrane depolarization. In Figure 3A, the K^+ current measured before addition of toxin (time 0) was

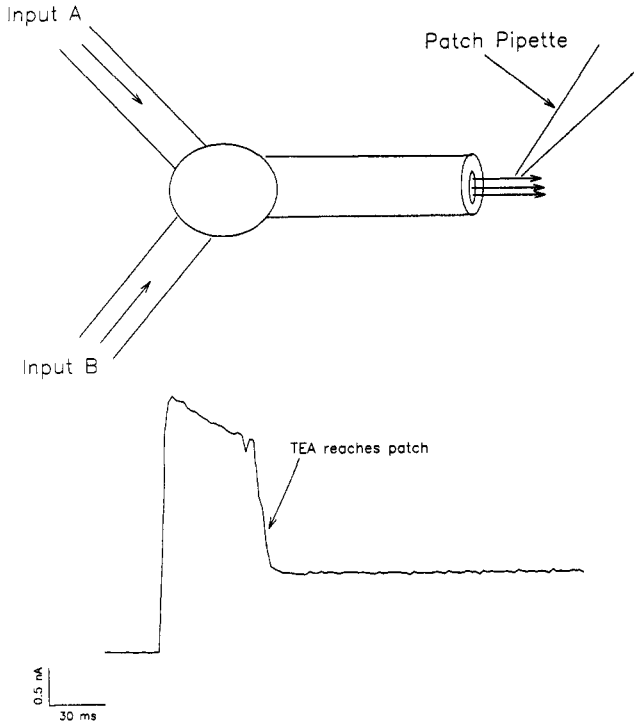

FIGURE 1: Outside-out membrane patches on the tip of a pipet are removed from *Xenopus* oocytes expressing Shaker K^+ channels and placed in the output stream of a continuously perfused capillary. The input flow is under computer control and can be switched between toxin-containing and control solutions. The current shown was elicited by depolarization of a patch containing several thousand Shaker K^+ channels. The pipet and bath solutions are as stated under Materials and Methods. At the onset of depolarization, the input was switched from control to a solution containing 30 mM tetraethylammonium chloride (added to the control solution) to block the channels partially. The inhibitor reaches the patch as a near-squarewave about 50 ms after the solution change.

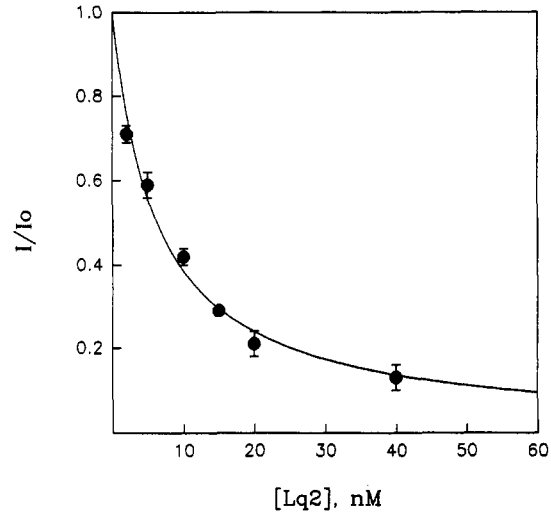

FIGURE 2: Equilibrium blockade of Shaker K^+ channels by Lq2. Shaker K^+ currents were measured in the absence (I_0) and in the presence (I) of various concentrations of Lq2. The unblocked fraction of channels, I/I_0, is plotted as a function of the Lq2 concentration. Each data point and standard error is based on three to five separate measurements. The solid curve corresponds to eq 3 with inhibition constant $K_i = \beta/\alpha = 6.9$ nM. These measurements were made on whole oocytes using a two-electrode voltage clamp amplifier (see Materials and Methods).

large. At sequential time points following abrupt exposure of the patch to 10 nM Lq2, the current became progressively smaller until an equilibrium level of channel inhibition was reached. Toxin produced a reduction of K^+ current that was constant throughout the duration of each depolarizing pulse.

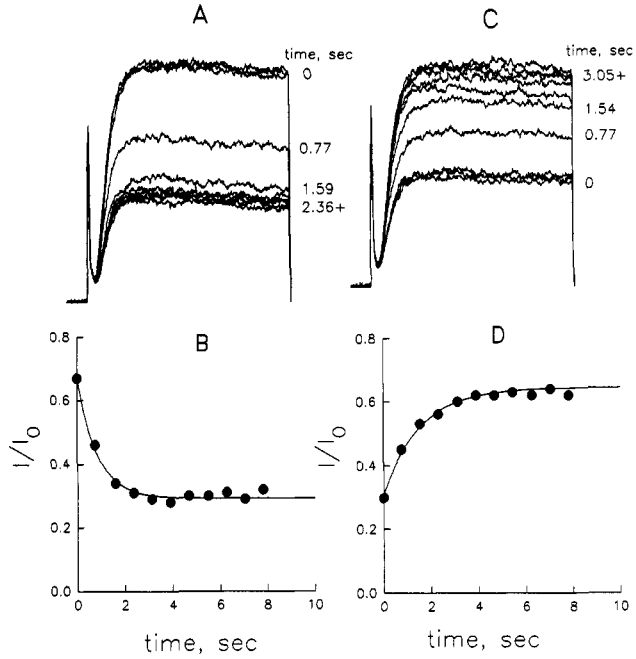

FIGURE 3: Determining rate constants from current relaxations to equilibrium. (A) A patch containing several hundred Shaker K^+ channels was repeatedly depolarized to 0 mV for 20 ms. After several traces were recorded in the absence of toxin (time = 0), solution containing 10 nM Lq2 was perfused. Time following addition of toxin is indicated beside each trace. (B) Normalized current amplitudes, I/I_0, from part A are plotted as a function of time. (C, D) The corresponding recovery time course following toxin removal from the same patch is shown. The solid curves in parts B and D correspond to eq 1–3 when $\alpha = 6.6 \times 10^7$ M^{-1} s^{-1} and $\beta = 0.57$ s^{-1} (B) or 0.64 s^{-1} (D).

This simple scaling down of the current stems from the fact that Lq2 inhibits a channel by binding to both the closed and open states. In these experiments, the toxin is binding to the closed state while the membrane is hyperpolarized: the depolarization is simply our way of looking at the unblocked fraction of channels. In Figure 3B, the current amplitude is plotted as a function of time; the current relaxes monotonically to an equilibrium level of blockade in about 3 s. Figure 3C,D shows the relaxation back to the initial fully unblocked level after toxin removal. The solid curves correspond to exponential relaxations characterized by eq 1, 2, and 3 with an association rate constant, α, of 6.6×10^7 M^{-1} s^{-1} and a dissociation rate constant, β, of 0.57 s^{-1} (estimated from panels A and B) or 0.64 s^{-1} (estimated from panels C and D).

To critically test whether Lq2 and the Shaker K^+ channel interact in a simple bimolecular fashion (the assumption of eq 1–3), the association and dissociation rate constants were determined as in Figure 3 using several toxin concentrations, and the results are shown in Figure 4. The dissociation rate constant is independent of toxin concentration, and the first-order association rate constant ($k_{on} = \alpha[T]$) increases linearly with toxin concentration. These findings are expected for a simple bimolecular reaction between the toxin and channel. Thus, a single toxin molecule diffuses up to and binds to the channel to induce the blocked state.

We are now in a position to ask the following: How does a charged residue on the ion channel near the toxin binding site influence the bimolecular kinetics of toxin blockade? Previous work has shown that the charge at position 422 on the Shaker K^+ channel affects the equilibrium binding of an Lq2 isoform (MacKinnon & Miller, 1989a). When the glutamate (negatively charged) present in the wild-type channel is changed to glutamine (neutral) or lysine (positive), the toxin affinity is diminished. Furthermore, the dependence

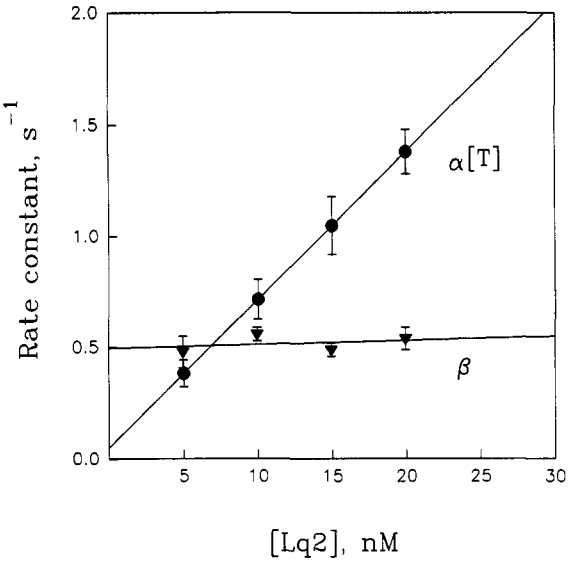

FIGURE 4: Concentration dependence of the rate constants. The Lq2 blocking kinetics were studied as shown in Figure 3 at several different toxin concentrations. The first-order rate constant α[T] for association (circles) and β for dissociation (triangles) are plotted as a function of the Lq2 concentration in nanomolar. The slope of the α[T] values corresponds to a second-order association rate constant $\alpha = 6.7 \times 10^7$ M^{-1} s^{-1}. The experimental conditions are described under Materials and Methods.

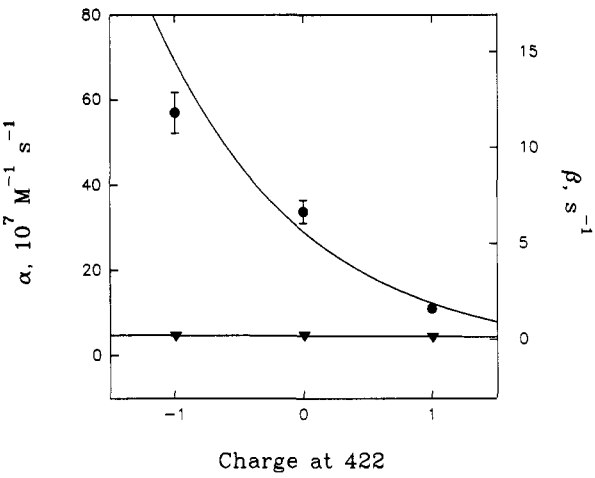

FIGURE 5: Association rate α is affected by charge-altering mutations at residue 422. Rate constants α (circles) and β (triangles) were determined as described in Figure 3 for wild-type Shaker K$^+$ channels and mutants with an altered charge at position 422. Plotted on the abscissa is the residue 422 electric charge (wild type, Glu = −1; mutant, Gln = 0, Lys = +1). These measurements were made in low ionic strength conditions with 25 mM bath NaCl. The solid curve overlying the α data corresponds to a theory in which the association rate constant is increased by the electrostatic potential at the toxin binding site (see Discussion). Debye–Huckel (linearized Poisson–Boltzmann) theory was used to relate the electrostatic potential to the channel charge density and electrolyte concentration. In the model, the electric potentials due to charges other than those at position 422 originate from a fixed charge placed 10 Å from the toxin binding site; the potential magnitude due to this "background" charge is −52 mV at 0 mM ionic strength. The 422 charge is placed 16 Å from the binding site and is adjusted according to the charge shown on the abscissa. The toxin valence is taken to be 4.5. The model is extremely oversimplified but shows that the data are consistent with an electrostatic interaction with charge screening.

of K_i on the charge at position 422 is quantitatively consistent with a Coulombic interaction with the cationic toxin.

Figure 5 and Table I show the effect of these charge-altering mutations on the association and dissociation rate constants for Lq2. A strikingly clean result is obtained: the mutations have a relatively large effect on the association rate (circles) and almost no effect on dissociation (triangles). In changing

Table I: Association Rate, α (M^{-1} s^{-1} × 10^{-7}), and Dissociation Rate, β (s^{-1}), for Channels with a Negative (Wild Type), Neutral (E422Q), and Positive (E422K) Charge at Residue 422[a]

		NaCl concentration, mM			
		25	50	100	200
wild type	α	56.9 ± 4.8	18.9 ± 2.7	8.5 ± 0.9	1.4 ± 0.1
	β	0.19 ± 0.012	0.32 ± 0.036	0.71 ± 0.07	1.07 ± 0.06
E422Q	α	33.8 ± 2.7	15.9 ± 0.5	3.95 ± 0.5	0.86 ± 0.06
	β	0.20 ± 0.02	0.23 ± 0.015	0.44 ± 0.034	0.81 ± 0.05
E422K	α	11.0 ± 1.0	5.5 ± 0.6	2.4 ± 0.2	0.61 ± 0.03
	β	0.13 ± 0.01	0.21 ± 0.02	0.36 ± 0.01	0.75 ± 0.04

[a] Rates were measured under the four ionic strength conditions shown. Each value is the mean ± SEM of three or more determinations.

residue 422 on the channel from glutamate to lysine, there is a 5-fold reduction (in 25 mM NaCl) of the association rate constant, α, while the dissociation rate constant, β, changes by a factor of less than 1.5.

We next studied the interplay between electrolyte concentration and the charge at position 422. Figure 6A shows α plotted as a function of the 422 charge. In one case, experiments were carried out under conditions of low ionic strength (25 mM NaCl; circles), and in another, 200 mM NaCl solutions were used (triangles). For each channel (negative, neutral, or positive charge at 422), raising the ionic strength caused a large reduction in the association rate. This fact is emphasized further in Figure 6B (also see Table I) where α is plotted as a function of the NaCl concentration. As the NaCl concentration is raised, α becomes smaller. The absolute reduction of α is of course greater in the channel with a negative charge at position 422. Also, from Table I it is evident that the relative reduction is also slightly greater. For example, note that the ratio α (wild type)/α (E422K) decreases as the NaCl concentration is raised. This finding is consistent with charge screening by electrolyte.

Although the toxin dissociation rate constant β did not depend significantly on the charge at 422, we did observe a dependence of β on the ionic strength (Figure 7). The toxin dissociates about 4 times faster when the ionic strength is raised from 25 to 200 mM. However, two features of this off-rate effect argue that it is independent of a simple electrostatic mechanism involving residue 422. First, β increases as a linear function of ionic strength over the range studied here, and second and most importantly, the ionic strength dependence is the same regardless of the charge at position 422. The lack of interaction between the 422 charge and the ionic strength-induced enhancement of the dissociation rate convinces us that the effect is independent of an electrostatic interaction between residue 422 and the toxin.

DISCUSSION

The scorpion toxin Lq2 inhibits the Shaker K$^+$ channel by binding to it in a simple bimolecular fashion. The ease with which channel inhibition can be measured using electrophysiological techniques allows one to study a docking interaction between two proteins at very high resolution. In this study, we address one central question: How does changing a charged residue on the ion channel near the toxin binding site affect the association and dissociation rates? As we discuss below, the way in which electrostatic potentials influence the two rates can provide detailed information about the steps which limit the rates of formation and breakdown of the toxin–channel complex.

The basic observation here is that charge-altering mutations introduced at position 422 on the channel influence only the association rate of the cationic toxin. As the 422 charge is

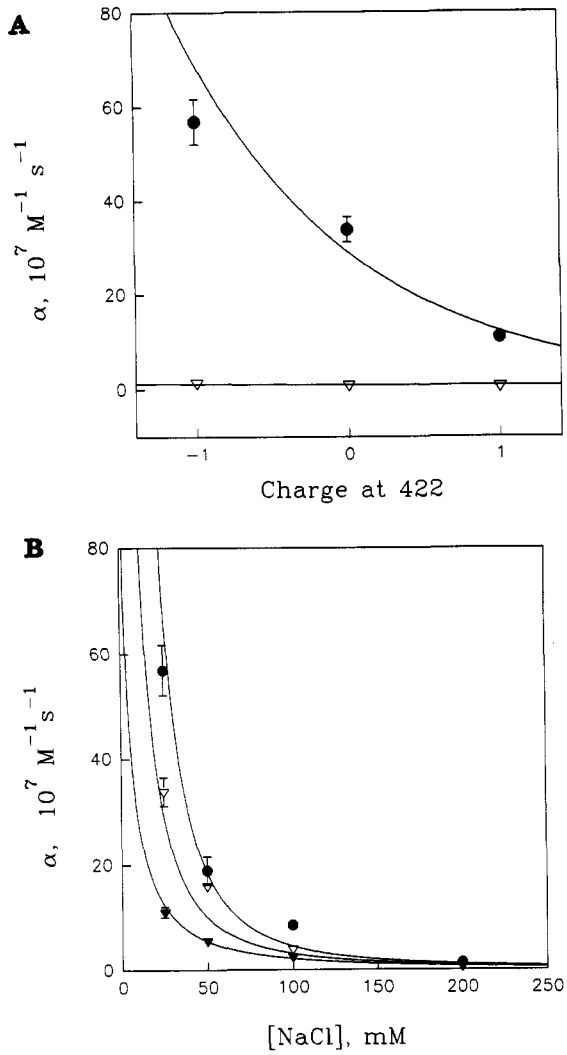

FIGURE 6: Effect of ionic strength on the association rate α in the different charge mutants. (A) α is plotted against the charge at position 422 for measurements made at low (25 mM NaCl; circles) and at high (200 mM NaCl; triangles) bath ionic strength. (B) α is plotted as a function of ionic strength (bath NaCl) for channels with a negative (circles), neutral (empty triangles), and positive (filled triangles) residue at position 422. The solid curves correspond to the model described in Figure 5 with adjustment of the 422 charge in part A or the ionic strength in part B. The association rate in the limit of very high ionic strength (or when the toxin charge is taken to be zero) is 10^6 M^{-1} s^{-1}. The bath solutions are as described under Materials and Methods.

changed incrementally from negative to positive, the association rate constant becomes smaller (Figure 5). The relationship between the ionic strength, the charge at position 422, and the association rate is qualitatively consistent with a through-solution electrostatic interaction between the cationic toxin and residue 422 on the channel. We therefore imagine that residue 422 is in close enough proximity to influence the electrostatic potential at the toxin binding site. Of course, the residue at 422 must contribute only a fraction of the total electrostatic interaction between the toxin and channel. After all, the ionic strength experiments reveal net electrostatic attraction even when a positive charge is placed at 422. Although the absolute numbers for toxin valence and distance between toxin and 422 used to fit the data cannot be taken seriously, the fits demonstrate a qualitative adherence of the data to a simple electrostatic theory which incorporates charge screening.

The toxin dissociation rate constant is relatively insensitive to our mutations at 422; nearly all of the electrostatic influence on the affinity is expressed in the association rate constant. Such an asymmetric effect of surface electrostatics on the kinetics of a protein–protein docking reaction has been observed for hemoglobin dimerization, where only the forward rate constant is affected by changes in surface charge density (Mrabet et al., 1986). The result can be rationalized by drawing a distinction between diffusional and nondiffusional steps in the bimolecular reaction (Schurr, 1970; Shoup & Szabo, 1982; Mrabet et al., 1986). In terms of the system under study here, the toxin must first diffuse up to its receptor site on the channel before it can bind. The binding step might involve the rearrangement of amino acid side chains, the displacement of hydration water, and perhaps the formation of hydrogen bonds necessary to produce the bound state. Similarly, dissociation must involve the disruption of favorable short-range interactions and then diffusion of toxin away from the receptor site. We therefore write the reaction between toxin (T), channel (C), and the bound state (B) as

$$T + C \underset{k_{-1}}{\overset{k_1}{\rightleftharpoons}} EC \underset{k_{-2}}{\overset{k_2}{\rightleftharpoons}} B$$

where the k_1 and k_{-1} transitions represent diffusion up to and away from an encounter complex (EC). The k_2 and k_{-2} transitions correspond to the final rearrangements which must be made in order to form the bound state. The encounter complex represents an infinite number of possible initial contact orientations formed between the toxin and channel. If we assume a steady-state condition for the concentration of encounter complex (Shoup & Szabo, 1982), then, according to our two-part reaction scheme, the association rate constant is given by

$$\alpha = k_1 k_2/(k_{-1} + k_2) \quad (4)$$

and the dissociation rate constant is

$$\beta = k_{-1} k_{-2}/(k_{-1} + k_2) \quad (5)$$

We next consider the case when $k_{-1} \gg k_2$). Equations 4 and 5 become

$$\alpha = k_1 k_2/k_{-1} \quad (6)$$

and

$$\beta = k_{-2} \quad (7)$$

Long-range electrostatic forces due to charges on the toxin and channel will be important in the steps where the two proteins (and thus the charges) move relative to each other. It is therefore reasonable to assume that the diffusion steps, k_1 and k_{-1} in our reaction scheme, should carry most of the electrostatic potential dependence. In general (eq 4 and 5) as well as in the diffusion-controlled limit ($k_2 \gg k_{-1}$), both α and β should be affected by local electrostatic potentials (Schurr, 1970). However, in the limit where $k_{-1} \gg k_2$, eq 6 and 7 show that k_1 and k_{-1} drop out of the expression for β. Thus, only the association rate constant α should be sensitive to the charge at position 422. An effect of local surface electrostatics on the association rate and not on the dissociation rate follows naturally if the rate-limiting steps in toxin binding occur after the toxin and channel come in contact.

In a previous study of ChTX blockade of a Ca^{2+}-activated K^+ channel, the association and dissociation rate constants were found to scale with the solution viscosity (Miller, 1990). ChTX and Lq2 are so similar that the results from the ChTX study probably apply to Lq2. However, viscosity-dependent rate constants would seem to be at odds with our findings here. The standard explanation for viscosity dependence requires the diffusion-controlled limit, that is, that $k_2 \gg k_{-1}$ in our reaction scheme (Miller, 1990; Schurr, 1970). In fact,

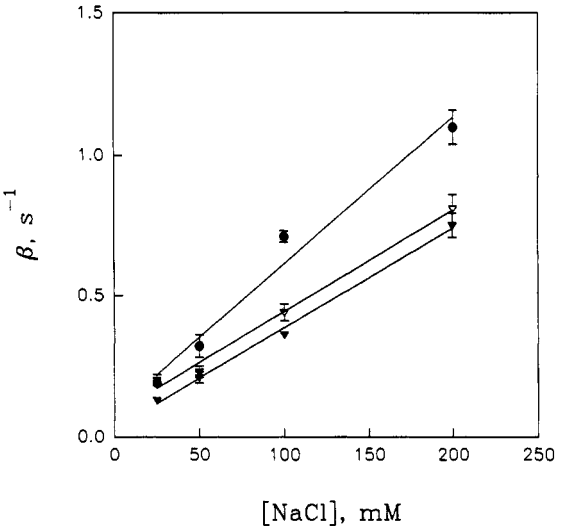

FIGURE 7: Toxin dissociation rate is affected by ionic strength. The dissociation rate constant, β, for channels with a negative (circles), neutral (triangles), and positive (filled triangles) residue at position 422 was measured at the different bath NaCl concentrations shown. Measurements were made as described in Figure 3.

viscosity dependence is generally assumed to be a diagnostic feature of a diffusion-controlled reaction, but for the case of two proteins docking, this assumption might not hold. Solution viscosity has been shown to influence the diffusion of small molecules within the interior of myoglobin (Beece et al., 1980; Barboy & Feitelson, 1989) as well as the rate of protein conformational changes within myoglobin (Ansari et al., 1992). Viscosity also can affect the rates of ion channel gating transitions (Shoukimas et al., 1981). These findings support the notion that intermolecular protein movements can be sensitive to solution viscosity. If indeed solution viscosity can influence the motion of side chains on the surface of a protein or even more global vibrations of a protein, then we might expect the k_2 and k_{-2} transitions in our reaction scheme to be viscosity-sensitive. In this case, our proposal that $k_{-1} \gg k_2$ (in order to account for an electrostatic effect isolated on the association rate) may not be inconsistent with viscosity-dependent rate constants. Experiments on the temperature dependence of toxin blocking kinetics will be needed to further test these ideas.

The details of the electrostatic interaction between Lq2 and the Shaker K^+ channel are obviously unknown. We have argued that, during its approach, the toxin senses the field due to a charge at 422, but what are the distances involved and how much of the toxin experiences the field? Park and Miller have shown for ChTX that several charges on the toxin can be neutralized without affecting the association rate or its ionic strength dependence (Park & Miller, 1992b). They point out that because the charges on the toxin are distributed over distances on the order of a Debye length, some residues are expected to contribute more than others to the overall electrostatic interaction. In the experiments carried out here, the ion channel is a homotetramer, and therefore a "single" 422 mutation alters the charge 4-fold. However, even in this setting of a more extensive charge density alteration, the interactions between nearby charged residues on the toxin and channel will probably dominate the electrostatic energy. With such paired interactions in mind, we next hope to identify complementary amino acids through mutagenesis of both the toxin and the channel.

ACKNOWLEDGMENT

We thank Jonathan Cohen and Chris Miller for their critical reviews of the manuscript.

REFERENCES

Anderson, C., MacKinnon, R., Smith, C., & Miller, C. (1988) *J. Gen. Physiol. 91*, 317–333.
Ansari, A., Jones, C. M., Henry, E. R., Hofrichter, J., & Eaton, W. A. (1992) *Science 256*, 1796–1798.
Barboy, N., & Feitelson, J. (1989) *Biochemistry 28*, 5450–5456.
Beece, D., Eisenstein, L., Frauenfelder, H., et al. (1980) *Biochemistry 19*, 5147–5157.
Botems, F., Roumestand, C., Gilquin, B., Menez, A., & Toma, F. (1991) *Science 254*, 1521–1523.
Catterall, W. A. (1988) *Science 242*, 50–61.
Galvez, A., Gimenez-Gallego, G., Reuben, J. P., et al. (1990) *J. Biol. Chem. 265*, 11083–11090.
Garcia, M. L., Galvez, A., Garcia-Calvo, M., King, V. F., Vazquez, J., & Kaczorowski, G. J. (1991) *J. Bioenerg. Biomembr. 23*, 615–646.
Giangiacomo, K. M., Garcia, M. L., & McManus, O. B. (1992) *Biochemistry 31*, 6719–6727.
Giangiacomo, K. M., Snugg, E. E., Garcia-Calvo, M., et al. (1993) *Biochemistry 32*, 2363–2370.
Gimenez-Gallego, G., Navia, M. A., Reuben, J. P., Katz, G. M., Kaczorowski, G. J., & Garcia, M. L. (1988) *Proc. Natl. Acad. Sci. U.S.A. 85*, 3329–3333.
Heginbotham, L., & MacKinnon, R. (1992) *Neuron 8*, 483–491.
Hoshi, T., Zagotta, W. N., & Aldrich, R. W. (1990) *Science 250*, 533–538.
Johnson, B. A., & Snugg, E. E. (1992) *Biochemistry 31*, 8151–8159.
Kamb, A., Iverson, L. E., & Tanouye, M. A. (1987) *Cell 50*, 405–413.
Kunkel, T. A. (1985) *Proc. Natl. Acad. Sci. U.S.A. 82*, 488–492.
Lucchesi, K., Ravindran, A., Young, H., & Moczydlowski, E. (1989) *J. Membr. Biol. 109*, 269–281.
MacKinnon, R., & Miller, C. (1988) *J. Gen. Physiol. 91*, 335–349.
MacKinnon, R., & Miller, C. (1989a) *Science 245*, 1382–1385.
MacKinnon, R., & Miller, C. (1989b) *Biochemistry 28*, 8087–8092.
MacKinnon, R., Reinhart, P. H., & White, M. M. (1988) *Neuron 1*, 997–1001.
MacKinnon, R., Heginbotham, L., & Abramson, T. (1990) *Neuron 5*, 767–771.
Miller, C. (1988) *Neuron 1*, 1003–1006.
Miller, C. (1990) *Biochemistry 29*, 5320–5325.
Miller, C., Moczydlowski, E., Latorre, R., & Phillips, M. (1985) *Nature 313*, 316–318.
Mintz, M. M., Adams, M. E., & Bean, B. P. (1992) *Neuron 9*, 85–95.
Moczydlowski, E., Lucchesi, K., & Ravindran, A. (1988) *J. Membr. Biol. 105*, 95–111.
Mrabet, N. T., McDonald, M. J., Turci, S., Sarkar, R., Szabo, A., & Bunn, H. F. (1986) *J. Biol. Chem. 261*, 5222–5228.
Park, C. S., & Miller, C. (1992a) *Neuron 9*, 307–313.
Park, C. S., & Miller, C. (1992b) *Biochemistry 31*, 7749–7755.
Park, C. S., Hausdorff, S. F., & Miller, C. (1990) *Proc. Natl. Acad. Sci. U.S.A.*
Sanger, F., Nicklen, S., & Coulson, A. R. (1977) *Proc. Natl. Acad. Sci. U.S.A. 74*, 5463–5467.
Schurr, J. M. (1970) *Biophys. J. 10*, 700–716.
Shoukimas, J. J., French, R. J., Belamarich, P., Brodwick, M. S., & Eaton, D. C. (1981) *Biophys. J. 33*, 282a.
Shoup, D., & Szabo, A. (1982) *Biophys. J. 40*, 33–39.
Smith, C., Phillips, M., & Miller, C. (1986) *J. Biol. Chem. 261*, 14607–14613.